



ELSEVIER

Contents lists available at ScienceDirect

Physica E

journal homepage: [www.elsevier.com/locate/physe](http://www.elsevier.com/locate/physe)

# Coulomb pseudogap in scattering-assisted tunneling of electrons between Landau-quantized two-dimensional electron gases

V.G. Popov<sup>a,b,\*</sup>, O.N. Makarovskiy<sup>c</sup>, V.T. Renard<sup>d</sup>, J.-C. Portal<sup>e,f,g</sup>

<sup>a</sup> Institute of Microelectronics Technology, RAS, Chernogolovka, Moscow District 142432, Russia

<sup>b</sup> Moscow Institute of Physics and Technology, Physical and Quantum Electronics Department Dolgoprudnyi, Moscow District 141700, Russia

<sup>c</sup> School of Physics and Astronomy of Nottingham University, Nottingham NG7 2RD, UK

<sup>d</sup> Néel Institute, CNRS, BP 166, F-38042, Grenoble Cedex 9, France

<sup>e</sup> GHMFL, CNRS, BP 166, F-38042, Grenoble Cedex 9, France

<sup>f</sup> INSA, 135 Avenue de Rangueil, F-31077 Toulouse Cedex 4, France

<sup>g</sup> Institut Universitaire de France, 103 Bd. St. Michel, F-75005 Paris, France

## ARTICLE INFO

### Article history:

Received 12 June 2010

Accepted 29 June 2010

Available online 21 July 2010

## ABSTRACT

We investigate electron tunneling between two GaAs accumulation two-dimensional layers separated by an (AlGa)As barrier which is modulation-doped with donors. A Coulomb pseudogap suppresses electron tunneling at the Fermi level and is induced by a magnetic field applied perpendicular to the accumulation layers. By measuring the tunnel current as a function of magnetic field and bias voltage, we examine how the pseudogap is influenced by elastic scattering processes.

© 2010 Elsevier B.V. All rights reserved.

## 1. Introduction

Many-body effects are the most attractive subjects of investigation in the modern semiconductor physics. In particular a two-dimensional electron gas (2DEGs) in a quantizing magnetic field is the most successive object for such a kind of investigation. Actually the electron transport in the gas reveals such many-body effects as the fractional quantum Hall effect, the Wigner crystallization, the skyrmion effects [1]. Now a lot of attention is paid to the many-body state of the 2DEG at the Landau-levels filling factor  $\nu = \frac{5}{2}$  [2]. Most of these effects are investigated experimentally by the in-plane electron transport. As for the tunneling, i.e., vertical electron transport, there were observed only few many-body effects concerning this activity. The first one was the Coulomb pseudogap [3]. The pseudogap causes suppression of electron tunneling at the Fermi level of the 2DEG, whereas the electron motion remains free along the plane of the 2DEGs. The physics of the pseudogap is similar to that of the Fermi-edge singularity [4]. Briefly speaking since electron tunneling is a fast process, it introduces a local charge fluctuation that is relaxed by the lateral motion of nearby electrons. In the presence of a magnetic field applied perpendicular to the 2DEG planes, the resulting vortex-like motion requires a finite amount of energy or pseudogap energy [5]. As a result, tunneling electrons encounter a pseudogap at the Fermi energy. The pseudogap has been observed as a suppression of the tunnel current between identical 2DEGs [6] at low bias or as an

additional voltage shift of the resonant current peak in the case of 2DEGs with different electron concentrations [7]. Recently an enhancement of the Landau levels (LL) spin-splitting was observed in electron tunneling between 2DEGs or in the 2D–2D tunneling [8]. The similar effect was observed earlier in the lateral transport and originated from the exchange part of the Coulomb interaction of the electrons in the 2DEGs. This splitting was found to be equal for the both gases in spite of its different filling factors that indicates on the gases should not be considered as separate systems concerning Coulomb electron interaction. It might be more appropriate to apply the physics of the bilayer 2DEGs for the 2D–2D tunnel structures. In addition the collapse of the spin-splitting was observed at  $\nu \leq 2$  [8] similar effect was observed in asymmetric double-quantum-well systems [9].

It is worth noting that the resonant character of the 2D–2D tunneling is very important for the pseudogap investigation. In the single-particle picture the tunnel current has a sharp peak when the subband levels align in both 2DEGs, i.e.,  $E_{01} = E_{02}$  (see insert in Fig. 1). This condition is a following of tunneling coherence, i.e., of the electron energy and transverse momentum conservation. In a quantizing magnetic field new current peaks appear in the  $I$ – $V$  curve. The peaks originate from the electron tunneling assisted by elastic scattering [10]. In this case the energy conservation gives additional resonant conditions as follows:

$$E_{01} - E_{02} = k\hbar\omega_c, \quad (1)$$

where  $k$  is an integer number,  $\hbar$  is the Planck constant,  $\omega_c$  is the cyclotron frequency. Thus elastic scattering assists electron tunneling between Landau levels (LLs) with the Landau level

\* Corresponding author at: Institute of Microelectronics Technology, RAS, Chernogolovka, Moscow District 142432, Russia. Tel.: +7 4965244016; fax: +7 4965244094.

E-mail address: [popov@iptm.ru](mailto:popov@iptm.ru) (V.G. Popov).

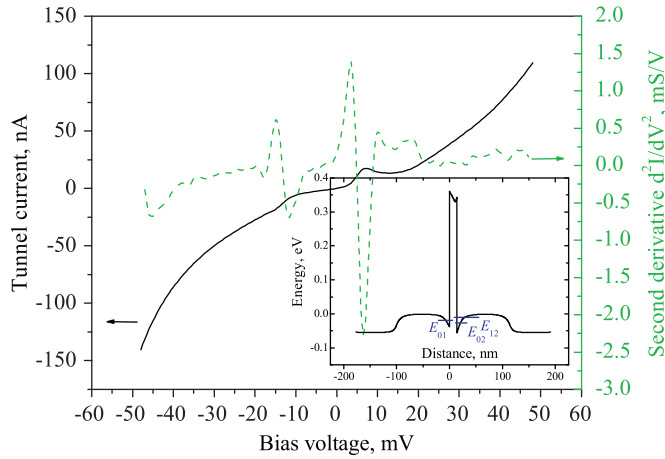


**Fig. 1.** Tunnel characteristics of the heterostructure under investigation. A solid curve shows the current–voltage characteristic of the diode; a dashed one corresponds to the second current derivative  $d^2I/dV^2$ . In the insert a schematic diagram of the conduction-band bottom plotted as a solid curve and the subband levels shown as solid segments.

number difference of  $k$ . Given that many-body effects cause a voltage shift of the resonance peak, it is interesting to pose the question “what happens to the elastic scattering features?” Here we study these elastic features in the  $I$ – $V$  curves for the case of 2D–2D electron tunneling at high magnetic fields,  $B$ , applied perpendicular to the 2DEG planes.

## 2. Experiment

Our single barrier GaAs/(AlGa)As/GaAs heterostructure was grown by molecular beam epitaxy on an  $n^+$ -Si-doped GaAs substrate and consists of two electron accumulation layers on either side of a single 20 nm thick barrier layer of  $\text{Al}_{0.3}\text{Ga}_{0.7}\text{As}$  which is modulation-doped with Si-donors near its centre. Accumulation 2D layers appear in the adjacent undoped GaAs layers due to the donor ionization in the barrier layer. In this case the 2DEGs are separated from the  $n^+$ -GaAs layers with spacers or doped 70 nm thick GaAs layers. A detailed description of the heterostructure can be found in Table 1. A schematic conduction band diagram of the diode is shown in the insert of Fig. 1. The structures were processed into mesa diodes using optical lithography and wet etching. The parameters of the 2DEGs are as follows: the concentration of the 2DEG with subband energy  $E_{01}$  is  $n_1 = 4 \times 10^{11} \text{ cm}^{-2}$ ; the concentration of the 2DEG accumulation layer with level  $E_{02}$  is  $n_2 = 6 \times 10^{11} \text{ cm}^{-2}$ .

According to the previous investigation [11] we can state that the resistance of the spacers is negligible in compare with that of the barrier layers. This allowed us to interpret all the features in the  $I$ – $V$  curve as features of 2D–2D electron tunneling. The parameters of the 2DEGs have been determined in the similar way as that was used in Ref. [8]. The tunnel characteristics were measured at temperature  $T = 1.5 \text{ K}$ . A typical current–voltage characteristic of the diode is shown in Fig. 1 as a solid curve. A current peak at the bias voltage  $V_r = 7 \text{ mV}$  corresponds to the first coherent resonance when the first resonant condition is satisfied, i.e.,  $E_{01}(V_r) = E_{02}(V_r)$ . A current shoulder at  $V_s = -14 \text{ mV}$  associates with the second resonance, i.e.,  $E_{01}(V_s) = E_{12}(V_s)$ . To improve energy resolution and to exclude influence of a non-resonant background current we have investigated the second derivative of the current on voltage shown in Fig. 1 as a dashed curve. In this case for the positive voltage the  $d^2I/dV^2$  minimum of the highest amplitude corresponds to the first resonance while for the negative voltage the  $d^2I/dV^2$  maximum of

**Table 1**

Layer sequence of the heterostructure under investigation.

Layer composition	Donor density ( $\text{cm}^{-3}$ )	Thickness (nm)
$n^+$ -GaAs (upper layer)	$1.5 \times 10^{18}$	300
$n^+$ -GaAs	$5 \times 10^{17}$	50
$n$ -GaAs (spacer)	$(2-3) \times 10^{15}$	70
GaAs	Undoped	10
$\text{Al}_{0.3}\text{Ga}_{0.7}\text{As}$	Undoped	5
$n^+$ - $\text{Al}_{0.3}\text{Ga}_{0.7}\text{As}$	$6 \times 10^{17}$	10
$\text{Al}_{0.3}\text{Ga}_{0.7}\text{As}$	Undoped	5
GaAs	Undoped	10
$n$ -GaAs (spacer)	$(2-3) \times 10^{15}$	70
$n^+$ -GaAs	$5 \times 10^{17}$	50
$n^+$ -GaAs	$1.5 \times 10^{18}$	1000

Substrate:  $n^+$ -GaAs,  $n_D = (2-3) \times 10^{18} \text{ cm}^{-3}$ .

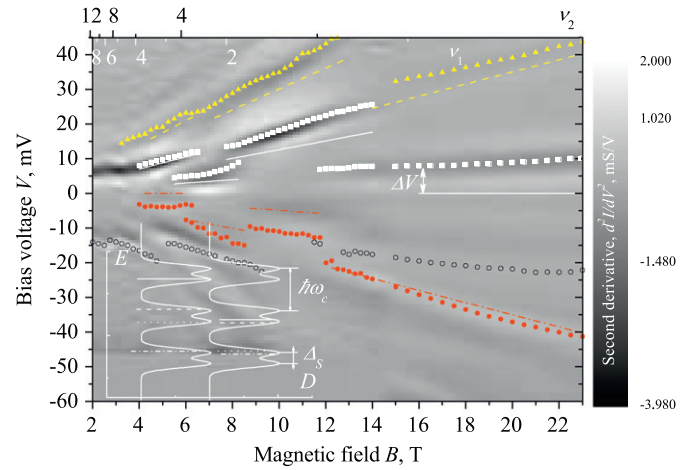


**Fig. 2.** Tunnel spectra for  $B$  applied perpendicular to the 2DEG planes. The grey-scale plot was reconstructed [16] from the original second derivative–voltage curves at different  $B$ . Filled square, circular, triangular and empty circular symbols show the experimental values of  $V_r$ ,  $V_{en}$ ,  $V_{ep}$  and  $V_s$  accordingly. This values are taken from the curves. The values of  $V_r$ ,  $V_{ep}$  and  $V_{en}$  calculated in the single-particle model are shown as segments of the solid, dashed and dash-dotted lines accordingly. In the insert the Landau levels in the 2DEGs are shown in an energy–density-of-states (E–D) plot. The LL are under first resonance condition in the case of the LL pinning. In this case segments of horizontal solid lines show the pinned Fermi levels in the 2DEGs in the magnetic field range  $4\text{T} < B < 6\text{T}$ . Horizontal segments of dashed lines correspond the Fermi levels in the magnetic field range  $6\text{T} < B < 8\text{T}$ . Segments of dotted lines show the Fermi levels in the magnetic field range  $9\text{T} < B < 14\text{T}$ . The Fermi levels in the field range  $B > 15\text{T}$  are shown as dot-dashed segments. The resonance voltage  $V_r$  is proportional to the Fermi level separation.

the highest amplitude associates to the second resonance (see Fig. 1). In a magnetic field applied perpendicular to the 2DEGs planes the current peak and shoulder are shifted and have non-monotonic magnetic field dependencies. In addition new features appear in the  $I$ – $V$  and in the  $d^2I/dV^2$ – $V$  curves (see grey-scale plot in Fig. 2).

## 3. Discussion

The non-monotonic voltage shift of the resonance features can be understood as follows. Above 2T, the Landau levels become well-defined and the energies of the subband levels oscillate as a function of  $B$ ; this modulation is induced by Landau level depopulation and a transfer of charge between the 2DEGs and the nearby doped GaAs contact layers and can be strong enough to provide LL pinning on the Fermi levels. The behaviour was calculated numerically [12] and observed by the optical [13] and

the capacitance [14] spectroscopy. The conditions of the LL pinning have been considered analytically in Ref. [15]. The subband level oscillations are similar to the Shubnikov–de Haas those in the sense that they are periodical in the inverse field and their period is determined by the Fermi energy at zero field or the electron concentration.<sup>1</sup> Since the concentrations of the 2DEGs are different the oscillations of the subband levels  $E_{01}$  and  $E_{02}$  are not in-phase. This means that the energy difference  $\Delta E = E_{01} - E_{02}$  is also oscillating and causes the oscillations of the first-resonance voltage  $V_r$ , i.e., the voltage at which  $\Delta E(V_r) = 0$ . To improve the experimental accuracy we have determined the resonant voltage as a voltage of the  $d^2I/dV^2$  minimum. The experimental values of the voltage  $V_r$  are plotted in Fig. 2 as filled squares. Similar behaviour has been observed previously [8]. We note that in the single-particle approximation, coherent resonance takes place when the Landau ladders of the 2DEGs coincide ( $k = 0$  in Eq. (1) see also insert in Fig. 2). If the upper partially filled LLs are pinned to the Fermi levels in both 2DEGs then the resonance voltages are determined by the energy difference of the upper partially filled LLs (see insert in Fig. 2). One can determine the quantum numbers of the upper LLs from the LL filling factors plotted on the top axis in Fig. 2. Hence for  $4\text{ T} < B < 6\text{ T}$ ,

$$eV_r = \hbar\omega_c, \quad (2)$$

for  $6\text{ T} < B < 8\text{ T}$ ,

$$eV_r = \Delta_s, \quad (3)$$

where  $\Delta_s$  is the LL spin splitting; for  $9\text{ T} < B < 14\text{ T}$ ,

$$eV_r = \hbar\omega_c - \Delta_s, \quad (4)$$

and for  $B > 15\text{ T}$ ,<sup>2</sup>

$$eV_r = 0. \quad (5)$$

We attribute the significant shift of the experimental data from the expected values to the effect of the Coulomb pseudogap. By plotting the difference  $\Delta V_r$  between the experimental and expected values we can describe empirically the data by a unified dependence over the full range of  $B$ —see circles in Fig. 3—using the relation

$$\Delta V_r = \beta + \sqrt{\alpha(B - B_0)}, \quad (6)$$

where  $\beta = 0.9\text{ mV}$ ,  $\alpha = 5.2 \times 10^{-6}\text{ V}^2/\text{T}$ ,  $B_0 = 6.5\text{ T}$  are the fitting parameters. The similar sublinear dependences were observed previously in the different structures and temperature [7,8]. To our knowledge there is no theory describing such magnetic dependence of the pseudogap shift. It is worth to note that the value of the LL spin splitting  $\Delta_s$  was chosen to succeed this unified-curve description. In this case we suppose that  $\Delta_s = 0.28\hbar\omega_c$ . This corresponds to the Landé factor of  $g^* = 8.4$ . This value is very close to the previous experimental observations of the exchange-enhanced Landé factor [17,18].

Thus we have the well-described magnetic dependence of the first coherent resonance in the frame of the LL pinning model. We shall show further how this model can describe the elastic features in the tunnel spectra. In Fig. 2, the experimental voltage positions of the elastic features in positive and negative bias are shown as triangles and circles. To calculate the positions of the elastic features in the single-particle model one should take into account the concentration corrections. Due to the finite

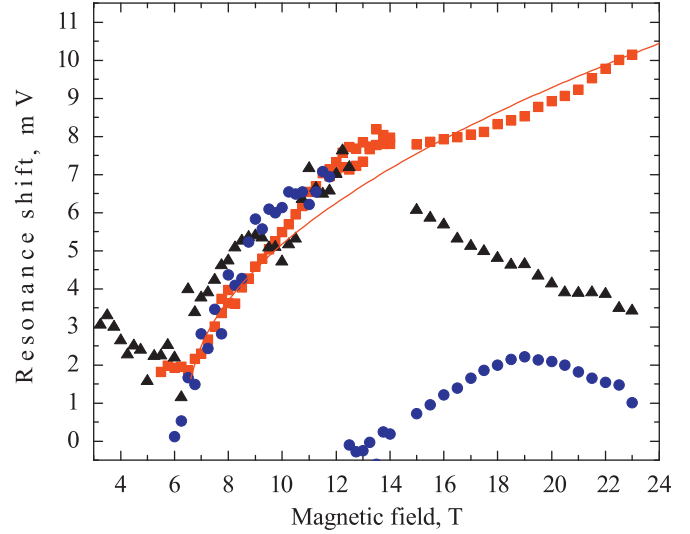


Fig. 3. Voltage shifts of the first and the elastic resonances at positive and negative bias are shown versus magnetic field as circles, squares and triangles accordingly. A solid line shows the best fit sublinear curve to the squares.

capacitance of the tunnel barrier an applied voltage changes the electron concentrations and the LL filling factors. Since the barrier is relatively thick this provides only a small correction to the initial concentrations.<sup>3</sup> In the case of the elastic feature at positive bias we have average concentrations as follows:  $n_1 = 3.6 \times 10^{11}\text{ cm}^{-2}$  and  $n_2 = 6.4 \times 10^{11}\text{ cm}^{-2}$ . From these concentrations one can recalculate new LL filling factors and determine the new resonance voltage  $V_r$  from (2), (4) and (6). Being determined from Eq. (1) as:  $eV_{ep} = eV_r + \hbar\omega_c$  the positive elastic feature voltage  $V_{ep}$  can be found as follows: in the field  $4.5\text{ T} < B < 6.5\text{ T}$

$$eV_{ep} = 2\hbar\omega_c, \quad (7)$$

for  $7\text{ T} < B < 11\text{ T}$

$$eV_{ep} = 2\hbar\omega_c - \Delta_s, \quad (8)$$

and for  $B > 13\text{ T}$

$$eV_{ep} = \hbar\omega_c. \quad (9)$$

The calculated values are shown in Fig. 2 as segments of dashed lines. One can see the considerable high-voltage shift of the experimental data with respect to the calculated those. In Fig. 3 this shift is plotted versus magnetic field. Note that this elastic pseudogap shift is very close to the shift of the first resonance at the magnetic field lower 12 T. However in the magnetic field higher 12 T it becomes considerably less than the coherent shift.

To understand what happens at  $B = 12\text{ T}$ , we consider the behaviour of the elastic feature in negative bias. The voltage positions  $V_{en}$  of the elastic feature are plotted in Fig. 2 as filled circles. The expected values are shown as segments of the dash-dotted lines and calculated taking into account the filling factors from Eq. (1) setting  $k = -1$  as follows: for  $4\text{ T} < B < 6\text{ T}$ ,

$$eV_{en} = 0, \quad (10)$$

<sup>1</sup> In our sample the spacers and barrier layers are thick enough to provide low value of the specific capacity that determines the number of electrons transferred from or in the 2DEG during these oscillations. This means that amplitude of the concentration oscillations is very small in compare with its average value.

<sup>2</sup> Here we have omitted the LL spin-splitting like it was done in Ref. [8]. Disappearance of the spin splitting will be discussed further when the elastic features will be considered.

<sup>3</sup> To calculate the concentration correction  $\Delta n$  one can use a specific capacitance of the barrier that is  $C = \epsilon\epsilon_0/d$ , where  $\epsilon = 13$  is the  $\text{Al}_{0.3}\text{Ga}_{0.7}\text{As}$  permittivity;  $\epsilon_0 = 8.9\text{ pF/m}$  is the vacuum permittivity;  $d$  is a thickness of the  $\text{Al}_{0.3}\text{Ga}_{0.7}\text{As}$  barrier layer. In this case  $\Delta n = V_a C/e$  where  $e$  is the electron charge;  $V_a$  is an average voltage position, relatively which the voltage position of a feature is changing in magnetic field. We can roughly estimate it for the elastic feature in positive bias as follows:  $V_a = (V_{ep}(B = 4.5\text{ T}) + V_{ep}(B = 23\text{ T}))/2$ . Finally the correction is  $\Delta n = 0.4 \times 10^{11}\text{ cm}^{-2}$ .

for  $6\text{T} < B < 8.5\text{T}$ ,

$$eV_{\text{en}} = \Delta_s - \hbar\omega_c, \quad (11)$$

for  $8.5\text{T} < B < 12\text{T}$ ,

$$eV_{\text{en}} = -\Delta_s, \quad (12)$$

and for  $B > 12\text{T}$ ,

$$eV_{\text{en}} = -\hbar\omega_c. \quad (13)$$

Similar to the positive elastic feature one can determine the shift of the elastic feature at negative bias. The experimental magnetic dependence of this shift are shown in Fig. 3 as filled circles. One can see that the elastic-feature shift starts to increase in the same field as the coherent-resonance one and sharply decreases at the field range  $B > 12\text{T}$ . This sharp decrease coincides with the second-resonance transition. In this transition the elastic feature is very close in the voltage position to the second resonance, i.e.,  $V_{\text{en}} \approx V_s$  (see Fig. 2) that means the cyclotron energy is close to the intersubband energy and it becomes larger in the higher field. It is interesting to note that the shift of the positive feature decreases at the same field  $B = 12\text{T}$ .<sup>4</sup> When the energy of a tunneling electron exceeds the intersubband that the electron can interact with the intersubband plasmon and relaxes more fast. Since the role of the plasmons is important in the pseudogap formation [5], pseudogap decrease can be associated with increasing role of the intersubband plasmon emission in the electron relaxation.

#### 4. Conclusions

To summarize the results, we have investigated the electron tunneling between 2DEGs of different concentrations in quantizing magnetic fields. The observed features have magnetic dependencies that can be explained in the model combining the LL pinning with such many-body effects as the Coulomb pseudogap and the enhanced LL spin-splitting. We revealed and investigated new effects such as the voltage shifts of the  $I$ - $V$

features created by the elastic scattering processes. These shifts significantly decrease in the high magnetic fields when the cyclotron energy exceeds the intersubband one. We ascribe this effect to the pseudogap formation in the case of fast electron relaxation via emission of the intersubband plasmons.

#### Acknowledgements

We acknowledge to A. Patane and to L. Eaves (Nottingham) for fruitful discussion and G. Hill (Sheffield University) for sample preparation. This work was supported by RFBR (Grant no. is 10-02-01318-a), EPSRC (UK) and CNRS/PICS (Grant no. is 3862).

#### References

- [1] S.D. Sarma, A. Pinczuk, Perspectives in Quantum Hall Effect, John Wiley & Sons, Inc., 1997.
- [2] C. Toke, N. Regnault, J.K. Jain, Phys. Rev. Lett. 98 (2007) 036806.
- [3] R.C. Ashoori, J.A. Lebens, N.P. Bigelow, R.H. Silsbee, Phys. Rev. Lett. 64 (1990) 681.
- [4] K.A. Matveev, A.I. Larkin, Phys. Rev. B 46 (1992) 15337.
- [5] I.L. Aleiner, H.U. Baranger, L.I. Glazman, Phys. Rev. Lett. 74 (1995) 3435.
- [6] J.P. Eisenstein, L.N. Pfeiffer, K.W. West, Phys. Rev. Lett. 69 (1992) 3804.
- [7] J.G.S. Lok, A.K. Geim, J.C. Maan, L. Eaves, A. Nogaret, P.C. Main, M. Henini, Phys. Rev. B 56 (1997) 1053.
- [8] V.G. Popov, Y.V. Dubrovskii, J.-C. Portal, JETP 102 (2006) 677.
- [9] Y. Takagaki, S. Tarucha, Semicond. Sci. Technol. 12 (1997) 715.
- [10] W. Demmerle, J. Smoliner, G. Berthold, E. Gornik, G. Weimann, W. Schlapp, Phys. Rev. B 44 (1991) 3090.
- [11] V. Popov, Ph.D. Thesis, Institute of Microelectronics Technology of RAS, 2001.
- [12] K.S. Chan, F.W. Sheard, G.A. Toombs, L. Eaves, Phys. Rev. B 56 (1997) 1447.
- [13] D.G. Hayes, M.S. Skolnick, D.M. Whittaker, P.E. Simmonds, L.L. Taylor, S.J. Bass, L. Eaves, Phys. Rev. B 44 (1991) R3436.
- [14] O.E. Dial, R.C. Ashoori, L.N. Pfeiffer, K.W. West, Nature 448 (2007) 176.
- [15] V.G. Popov, Phys. Rev. B 73 (2006) 125310.
- [16] R.J. Renka, A.K. Cline, Rocky Mountain J. Math. 14 (1984) 223.
- [17] A. Usher, R.J. Nicholas, J.J. Harris, C.T. Foxon, Phys. Rev. B 41 (1990) 1129.
- [18] V.T. Dolgoplov, A.A. Shashkin, A.V. Aristov, D. Schmarek, W. Hansen, J.P. Kotthaus, M. Holland, Phys. Rev. Lett. 79 (1997) 729.

<sup>4</sup> Here one can find another confirmations of the spin-splitting suppression. In the field  $B > 16\text{T}$  the spin polarisation of the pined LLs becomes different in the 2DEGs, i.e.,  $\nu_2 > 1$  and  $\nu_1 < 1$ . This means that Eq. (3) is valid again. Thus firstly we should observe the resonance transition at  $B = 16\text{T}$  but we do not. Secondly for the elastic features Eq. (11) and  $eV_{ep} = \hbar\omega_c + \Delta_s$  should be justified. In this case the single-particle  $V_{ep}$  values will exceed the experimental those that contradicts to the pseudogap effect and hardly can be explained.